

Exploiting persymmetry for low-rank Space Time Adaptive Processing

Guillaume Ginolhac, Philippe Forster, Frédéric Pascal, Jean-Philippe Ovarlez

▶ **To cite this version:**

Guillaume Ginolhac, Philippe Forster, Frédéric Pascal, Jean-Philippe Ovarlez. Exploiting persymmetry for low-rank Space Time Adaptive Processing. Signal Processing, 2014, 97 (4), pp.242-251. 10.1016/j.sigpro.2013.10.026 . hal-00926260

HAL Id: hal-00926260
https://hal.science/hal-00926260

Submitted on 9 Jan 2014

HAL is a multi-disciplinary open access archive for the deposit and dissemination of scientific research documents, whether they are published or not. The documents may come from teaching and research institutions in France or abroad, or from public or private research centers.

L'archive ouverte pluridisciplinaire **HAL**, est destinée au dépôt et à la diffusion de documents scientifiques de niveau recherche, publiés ou non, émanant des établissements d'enseignement et de recherche français ou étrangers, des laboratoires publics ou privés.

Exploiting Persymmetry For Low-Rank Space Time Adaptive Processing

G. Ginolhac, P. Forster, F. Pascal and J. P. Ovarlez[1]

LISTIC, Université de Savoie, B.P. 80439 74944 Annecy le Vieux Cedex, France

SATIE, ENS Cachan, CNRS, UniverSud, 61, av President Wilson, F-94230 Cachan, France

SONDRA, Supelec, Plateau du Moulon, 3 rue Joliot-Curie, F-91192 Gif-sur-Yvette CEDEX, France

ONERA, DEMR/TSI, Chemin de la Hunière, F-91120 Palaiseau, France

Abstract

Reducing the number of secondary data used to estimate the Covariance Matrix (CM) for Space Time Adaptive Processing (STAP) techniques is still an active research topic. Within this framework, the Low-Rank (LR) structure of the clutter is well-known and the corresponding LR STAP filters have been shown to exhibit a smaller Signal Interference plus Noise Ratio (SINR) loss than classical STAP filters, only $2r$ secondary data (where r is the clutter rank) instead of $2m$ (where m is the data size) are required to reach the classical 3dB SNR loss. By using other features of the radar system, other properties of the CM can be exploited to further reduce the number of secondary data: this is the case for active systems using a symmetrically spaced linear array with constant pulse repetition interval, which results in a persymmetric structure of the noise CM. In this context, we propose to combine this property of the CM and the LR structure of the clutter to perform CM estimation. In this paper, the resulting STAP filter is shown, both theoretically and experimentally, to exhibit good performance with fewer secondary data: 3dB SINR loss is achieved with only r secondary data.

Keywords: STAP, Low-Rank clutter, Persymmetry, Perturbation Analysis, SIRV.

Email address:
guillaume.ginolhac@univ-savoie.fr;pforster@u-paris10.fr;frederic.pascal@supelec.fr;o
(G. Ginolhac, P. Forster, F. Pascal and J. P. Ovarlez)

1. Introduction

Space Time Adaptive Processing (STAP) is a technique used in airborne phased array radar to detect moving target embedded in an interference background such as jamming or strong clutter [1]. While conventional radars are capable of detecting targets both in the time domain related to target range and in the frequency domain related to target velocity, STAP uses an additional domain (space) related to the target angular localization. The consequence is a two-dimensional adaptive filtering technique which uses jointly temporal and spatial dimensions to cancel interference and to improve target detection. In most works on radar, the clutter is assumed to be a simple Gaussian process. However, the increase of the radar resolution leads to a higher scene heterogeneity where the clutter can be no longer modeled by a Gaussian process [2, 3]. To take this heterogeneity into account, one can use the so-called Spherically Invariant Random Vector (SIRV) product model, first introduced by Yao [4] in the information theory community. This is a compound-Gaussian model, well-known for its good statistical properties and for its good fit to several real data sets [5, 6]. Secondly in side-looking STAP (as considered in this paper), the ground clutter can be shown to have a Low Rank (LR) structure from Brennan's rule [7]. Therefore, we decide to use the same disturbance model as in [8]: the disturbance is assumed to be the sum of a LR-SIRV clutter and a zero-mean white Gaussian noise.

In practice, the disturbance Covariance Matrix (CM) is generally unknown and an estimate is required to perform the STAP processing. This estimation procedure is currently performed by the Sample Covariance Matrix (SCM) built from the so-called secondary data, i.e. independent signal-free observations of the noise sharing the same distribution as the observation under test. In a STAP framework, the dimension of the CM can be important (the number of sensors times the number of pulses). Commonly, the number of secondary data has to be more than twice this dimension to ensure the classical 3dB loss on the performance results [9]. Several methods, denoted as reduced-rank, are proposed in STAP to reduce this number of secondary data. The first one, denoted LR-STAP filter, is based on a Singular Value Decomposition (SVD) of the SCM which is known to preserve such a performance of 3 dB loss [10, 11, 12, 13] for few secondary data. Moreover, in the context of a LR-SIRV clutter plus white Gaussian noise, results of [14] shows that the LR-STAP filer built from SCM allows to reach the same performance than in a Gaussian context[1]. To avoid the compu-

[1] LR-STAP filters built from other estimators (like for instance Normalized SCM) are less per-

tation of the SVD and to limit the computational time, some algorithms [15, 16] based on subspace tracking has been proposed. Similarly, to fill these gaps, new STAP algorithms based on a projection received data onto a lower dimensional Krylov subspace [17, 18, 19, 20] or based on joint iterative optimization of adaptive filters [21, 22] have been recently developed [2]. In this paper, we derive a new STAP filter from the SVD of a new estimator of the CM in order to still reduce the number of secondary data by reaching the same performance. Indeed, it is well known in array processing and particularly in radar systems (and STAP) to have a symmetrically spaced linear array for spatial domain processing, and/or symmetrically spaced pulse train for temporal domain processing [25, 26, 27] which leads to a particular structure of the disturbance CM: the persymmetric structure. It is well known that this persymmetric structure could be exploited to improve the estimation accuracy (or to reduce the number of secondary data to reach equivalent performance). In particular, the persymmetric Maximum Likelihood Estimate (MLE) of the disturbance CM is used instead of the SCM [28, 29] to improve the performance of adaptive detectors. But in a Low-Rank context, this persymmetric structure is not used in detectors or STAP filters.

We propose in this paper to build the projector onto the clutter subspace from this MLE which results in a new LR-STAP filter. We expect to achieve the classical 3dB loss for the performance results for a number of secondary data smaller than in classical LR-STAP filters. For this purpose, we investigate the theoretical Signal Interference plus Noise Ratio (SINR) Loss of this new LR-STAP filter in a LR-SIRV clutter plus white Gaussian noise context. Under the two hypotheses of LR-Gaussian clutter plus noise and orthogonality between the target signal and the clutter subspace, the theoretical analysis of LR-STAP filters has been conducted in the seminal works [10, 12, 13]. In [14], the first hypothesis has been relaxed and consequently the much more realistic case of a LR-SIRV clutter plus white Gaussian noise is considered. However, for mathematical tractability the second hypothesis was kept. In this paper, we extend these results by integrating the persymmetric property of the disturbance CM to investigate the theoretical SINR Loss of the new LR-STAP filter. Numerical simulations validate our results. Moreover for the theoretical SINR Loss computed from the proposed LR-STAP filter and the one in [14], several simulations that show the limits of validity are presented in this paper for various parameters:

---

formant.

[2] It is also possible to develop STAP algorithms robust to outliers as in [23, 24]

- hypothesis of orthogonality between the target signal and the clutter subspace,
- the texture distribution,
- the Clutter to Noise Ratio (CNR).

These simulations show that theoretical results of this paper and the ones of [14] are still valid for large values of texture, CNR and even when the assumption of orthogonality is not true anymore. Finally, these results show the interest of the combination of LR techniques and persymmetric property: the new STAP filter requires twice less secondary data than the classical LR-STAP filter for achieving equivalent performance. Moreover, the good performance of the new LR STAP filter is illustrated on STAP data composed of a real clutter and synthetic targets.

This paper is an extension of [30] with the details of the proof to obtain the theoretical SINR Loss. Moreover, several new simulations on simulated and real data have been done.

The paper is organized as follows: section 2 gives the problem statement and the definition of the Low-Rank STAP filter, section 3 contains the derivation of the corresponding theoretical SINR Loss and finally section 4 shows STAP simulations which illustrate the theoretical results. The following convention is adopted: italic indicates a scalar quantity, lower case boldface indicates a vector quantity and upper case boldface a matrix. ^{T} denotes the transpose operator, ^{H} the transpose conjugate and * the conjugate operator. $E[\,]$ is the expected value operator. $\mathscr{CN}(\mathbf{a}, \mathbf{M})$ is a complex Gaussian vector of mean $\mathbf{a}$ and of covariance matrix $\mathbf{M}$. $\mathbf{I}_m$ is the $m \times m$-identity matrix. $\chi^2(n)$ is a Chi-square random variable with n degrees of freedom.

2. Low-Rank STAP filter

2.1. Signal Model

STAP [1] is applied to airborne radar in order to detect moving targets. Typically, the radar receiver consists in an uniform linear array of N antenna elements processing M pulses in a coherent processing interval. In the following, let us set $m = NM$. In this framework, we assume that a known complex signal $\mathbf{d}$ corrupted by an additive disturbance $\mathbf{n}$ is in $\mathbf{x} \in \mathbb{C}^m$:

$$\mathbf{x} = \alpha\mathbf{d} + \mathbf{n}, \tag{1}$$

where α is a complex attenuation. We assume to have K secondary data $\mathbf{x}_k$ which only contain the disturbance:

$$\mathbf{x}_k = \mathbf{n}_k \;\; k = 1, \ldots, K \tag{2}$$

Moreover, it is assumed that $\mathbf{n}$ and $\mathbf{n}_k$ are independent and share the same statistical distribution and are modeled as the sum of a clutter, $\mathbf{c}$ or $\mathbf{c}_k$, and a white Gaussian noise, $\mathbf{b}$ or $\mathbf{b}_k$:

$$\begin{array}{rcl} \mathbf{n} & = & \mathbf{c} + \mathbf{b} \\ \mathbf{n}_k & = & \mathbf{c}_k + \mathbf{b}_k \quad k = 1, \ldots, K \end{array} \tag{3}$$

The processes $\mathbf{b}$ and $\mathbf{b}_k$ are modeled as zero-mean complex Gaussian noises, denoted by $\mathbf{b}\,,\ \mathbf{b}_k \sim \mathscr{CN}(\mathbf{0}, \lambda \mathbf{I}_m)$ ($\mathbf{I}_m$ is the identity matrix of size m). Concerning the clutter $\mathbf{c}$ and $\mathbf{c}_k$, we consider that their power in each cell k and the cell under test is different. In such a situation, it is common to model this kind of clutter by a SIRV [31]. A SIRV is a non-homogeneous Gaussian random vector with random power: its randomness is induced by spatial variation in the radar backscattering. The SIRV [4] $\mathbf{c}$ (resp. $\mathbf{c}_k$) is the product of a positive random variable τ (resp. τ_k), called the *texture*, and a m-dimensional independent complex Gaussian vector $\mathbf{g}$ (resp. $\mathbf{g}_k$), called the *speckle*, denoted by $\mathbf{g}\,,\ \mathbf{g}_k \sim \mathscr{CN}(\mathbf{0}, \mathbf{C})$ with zero-mean and CM $\mathbf{C} = E(\mathbf{g}\mathbf{g}^H) = E(\mathbf{g}_k \mathbf{g}_k^H)$:

$$\begin{array}{rcl} \mathbf{c} & = & \sqrt{\tau}\mathbf{g} \\ \mathbf{c}_k & = & \sqrt{\tau}_k \mathbf{g}_k \quad k = 1, \ldots, K \end{array} \tag{4}$$

In classical STAP context, we are able to evaluate the clutter rank thanks to the Brennan's rule [7] which leads to a low rank structure for the STAP clutter $\mathbf{c}$ and $\mathbf{c}_k$, e.g. rank $(\mathbf{C}) = r \ll m$. The *speckle* CM, $\mathbf{C}$, can be thus decomposed as:

$$\mathbf{C} = \sum_{i=1}^{r} \lambda_i \mathbf{u}_i \mathbf{u}_i^H \tag{5}$$

where $\lambda_1 > \lambda_2 > \ldots > \lambda_r > \lambda_{r+1} = \ldots = \lambda_{NM} = 0$ are the eigenvalues of $\mathbf{C}$ and $\{\mathbf{u}_1, \ldots, \mathbf{u}_r, \mathbf{u}_{r+1}, \ldots, \mathbf{u}_{NM}\}$ are the associated eigenvectors. The CM of $\mathbf{n}$ and $\mathbf{n}_k$ is then given by:

$$\mathbf{\Sigma} = E[\tau]\mathbf{C} + \lambda \mathbf{I}_m \tag{6}$$

Furthermore, many applications can result in a CM that exhibits some particular structure. For radar systems using a symmetrically spaced linear array for

spatial domain processing, and/or symmetrically spaced pulse train for temporal domain processing [25, 26, 27], the CM $\mathbf{\Sigma}$ has the persymmetric property which can be written as follows:

$$\mathbf{\Sigma} = \mathbf{J}_m \mathbf{\Sigma}^* \mathbf{J}_m, \tag{7}$$

where $\mathbf{J}_m$ is the m-dimensional antidiagonal matrix having 1 as non-zero elements. Since the signal vector is also persymmetric, one has:

$$\mathbf{d} = \mathbf{J}_m \mathbf{d}^* \tag{8}$$

One way to take advantage of the persymmetric property is to transform the complex primary data (1) and secondary data (2) into real data. The persymmetric operation can be characterized by an unitary matrix $\mathbf{T}$ defined as:

$$\mathbf{T} = \begin{cases} \frac{1}{\sqrt{2}} \begin{pmatrix} \mathbf{I}_{m/2} & \mathbf{J}_{m/2} \\ i\mathbf{I}_{m/2} & -i\mathbf{J}_{m/2} \end{pmatrix} & \text{for } m \text{ even} \\ \frac{1}{\sqrt{2}} \begin{pmatrix} \mathbf{I}_{(m-1)/2} & 0 & \mathbf{J}_{(m-1)/2} \\ 0 & \sqrt{2} & 0 \\ i\mathbf{I}_{(m-1)/2} & 0 & -i\mathbf{J}_{(m-1)/2} \end{pmatrix} & \text{for } m \text{ odd} \end{cases} \tag{9}$$

By applying the transformation $\mathbf{T}$ to all the quantities, one obtains:

$$\begin{array}{rcl} \mathbf{x}' & = & \mathbf{T}\mathbf{x} \\ \mathbf{x}'_k & = & \mathbf{T}\mathbf{x}_k \\ \mathbf{d}' & = & \mathbf{T}\mathbf{d} \\ \mathbf{c}' & = & \mathbf{T}\mathbf{c} \\ \mathbf{c}'_k & = & \mathbf{T}\mathbf{c}_k \\ \mathbf{b}' & = & \mathbf{T}\mathbf{b} \\ \mathbf{b}'_k & = & \mathbf{T}\mathbf{b}_k \end{array} \tag{10}$$

Let us remind that the transformed data are denoted thanks to a $'$ and, more importantly, that they are all real-valued, contrary to the original data which are complex-valued. The primary and the secondary data (1), (2) become after transformation by $\boldsymbol{T}$:

$$\begin{array}{rcll} \mathbf{x}' & = & \alpha\mathbf{d}' + \mathbf{c}' + \mathbf{b}' & \\ \mathbf{x}'_k & = & \mathbf{c}'_k + \mathbf{b}'_k & k = 1, \ldots, K \end{array} \tag{11}$$

The CM of data (11) is thus $\mathbf{\Sigma}' = \mathbf{T}\mathbf{\Sigma}\mathbf{T}^H$ and its eigendecomposition is given by:

$$\begin{array}{rcl} \mathbf{\Sigma}' & = & \sum_{i=1}^{r} E[\tau]\lambda_i \mathbf{u}'_i \mathbf{u}'^H_i + \lambda \sum_{i=1}^{m} \mathbf{u}'_i \mathbf{u}'^H_i \\ & = & \mathbf{S}'_\Sigma + \lambda \mathbf{I}_m \end{array} \tag{12}$$

where $\left\{\mathbf{u}'_1, \ldots, \mathbf{u}'_r, \mathbf{u}'_{r+1}, \ldots, \mathbf{u}'_m\right\}$ are the eigenvectors of $\mathbf{\Sigma}'$. Let us notice that the matrix covariance rank and the eigenvalues are unchanged by the operator $\mathbf{T}$.

Let us now define the projector onto the clutter subspace $\mathbf{\Pi}'_c$ and the projector onto the orthogonal of the clutter subspace $\mathbf{\Pi}'^{\perp}_c$ [10, 12]:

$$\begin{aligned} \mathbf{\Pi}'_c &= \sum_{i=1}^{r} \mathbf{u}'_i \mathbf{u}'^H_i \\ \mathbf{\Pi}'^{\perp}_c &= \mathbf{I}_m - \mathbf{\Pi}'_c \end{aligned} \tag{13}$$

2.2. Optimal and Sub-optimal STAP filters

The optimal STAP filter is known to be defined as [1]:

$$\mathbf{w}'_{opt} = \mathbf{\Sigma}'^{-1}\mathbf{d}', \tag{14}$$

whereas in LR assumption, it is expressed as [10, 12]:

$$\mathbf{w}'_{lropt} = \mathbf{\Pi}'^{\perp}_c \mathbf{d}' \tag{15}$$

In practical cases, since the CM $\mathbf{\Sigma}'$ (and therefore also $\mathbf{\Pi}'_c$) is unknown, it is necessary to estimate them from the secondary data $\mathbf{x}'_k$ (11).

This estimation is classically performed by using the SCM, but the persymmetric structure of $\mathbf{\Sigma}$ could be exploited to improve the estimation quality. The persymmetric MLE of the CM could be used instead of the SCM. The MLE, denoted $\hat{\mathbf{R}}'$, has been derived in [28, 29] and is given by:

$$\hat{\mathbf{R}}' = \mathcal{R}e(\mathbf{T}\hat{\mathbf{R}}_{SCM}\mathbf{T}^H) \tag{16}$$

where $\hat{\mathbf{R}}_{SCM}$ is the SCM computed from the original data (2) as follows: $\hat{\mathbf{R}}_{SCM} = \frac{1}{K}\sum_{k=1}^{K} \mathbf{x}_k \mathbf{x}_k^H$. From the eigenvectors $\{\hat{\mathbf{u}}'_1, \ldots, \hat{\mathbf{u}}'_m\}$ of $\hat{\mathbf{R}}'$, the estimates of the projectors (onto the subspace clutter and its complement) by using the persymmetric structure of the CM are defined as [10, 12]:

$$\begin{aligned} \hat{\mathbf{\Pi}}'_c &= \sum_{i=1}^{r} \hat{\mathbf{u}}'_i \hat{\mathbf{u}}'^H_i \\ \hat{\mathbf{\Pi}}'^{\perp}_c &= \mathbf{I}_m - \hat{\mathbf{\Pi}}'_c \end{aligned} \tag{17}$$

Finally, the adaptive filter $\hat{\mathbf{w}}'$ studied in this paper is:

$$\hat{\mathbf{w}}' = \hat{\mathbf{\Pi}}'^{\perp}_c \mathbf{d}' \tag{18}$$

The next section is devoted to the derivation of its theoretical performance.

3. Theoretical SINR Loss

3.1. Definition of the SINR Loss

As in previous works on LR-STAP theoretical performance analysis [12], the following usual assumption is made for mathematical tractability: the projection of the steering vector on the true interference subspace is negligible, i.e. $\mathbf{u}_i'^H \mathbf{d}' \approx 0$ for $i = 1, \ldots, r$. This just means that the target is not fully embedded in the clutter ridge. In the next section, simulations will show that the theoretical result is still valid in the case of non orthogonality between the target signal and the clutter subspace. From this assumption and from the structure of $\mathbf{\Sigma}'$, one has:

$$\mathbf{S}'_{\Sigma}\mathbf{d}' = \mathbf{\Pi}'_c\mathbf{d}' = \mathbf{0} \tag{19}$$

It follows from (12) and (13) that

$$\begin{array}{rcl} \mathbf{\Sigma}'\mathbf{d}' & = & \lambda\mathbf{d}' \\ \mathbf{\Sigma}'^{-1}\mathbf{d}' & = & \frac{1}{\lambda}\mathbf{d}' \\ \mathbf{\Pi}_c'^{\perp}\mathbf{d}' & = & \mathbf{d}' \end{array} \tag{20}$$

The generic STAP filter output is given by:

$$\mathbf{w}'^H\mathbf{x}' = \alpha\mathbf{w}'^H\mathbf{d}' + \mathbf{w}'^H\mathbf{n}' \tag{21}$$

The SINR at the filter output $SINR_{out}$ is:

$$SINR_{out} = \frac{|\alpha|^2|\mathbf{w}'^H\mathbf{d}'|^2}{E\left[\mathbf{w}'^H\mathbf{n}'\mathbf{n}'^H\mathbf{w}'\right]} = \frac{|\alpha|^2|\mathbf{w}'^H\mathbf{d}'|^2}{\mathbf{w}'^H\mathbf{\Sigma}'\mathbf{w}'} \tag{22}$$

$SINR_{out}$ is maximum when $\mathbf{w}' = \mathbf{w}'_{opt}$ and its value is:

$$SINR_{max} = |\alpha|^2\mathbf{d}'^H\mathbf{\Sigma}'^{-1}\mathbf{d}' \tag{23}$$

The SINR loss, denoted by ρ, is the loss of performance when $\mathbf{w}' = \hat{\mathbf{w}}'$ and it can be written as:

$$\rho = \frac{SINR_{out}}{SINR_{max}} = \frac{|\hat{\mathbf{w}}'^H\mathbf{d}'|^2}{\left(\hat{\mathbf{w}}'^H\mathbf{\Sigma}'\hat{\mathbf{w}}'\right)\left(\mathbf{d}'^H\mathbf{\Sigma}'^{-1}\mathbf{d}'\right)}. \tag{24}$$

From Eqs. (18), (19) and (20) the SINR loss, ρ can be rewritten as follows:

$$\rho = \frac{SINR_{out}}{SINR_{max}} = \lambda\frac{\left(\mathbf{d}'^H\hat{\mathbf{\Pi}}_c'^{\perp}\mathbf{d}'\right)^2}{\mathbf{d}'^H\hat{\mathbf{\Pi}}_c'^{\perp}\mathbf{\Sigma}'\hat{\mathbf{\Pi}}_c'^{\perp}\mathbf{d}'} \tag{25}$$

The next subsection is devoted to the derivation of the SINR Loss by using a perturbation analysis, known to be valid for large K.

3.2. Perturbation Analysis

The main result is given by the following proposition.

Proposition 3.1.

$$E\left[\rho\right] = 1 - \frac{1}{K'}\sum_{i=1}^{r}\left(\frac{E\left[\tau\right]\lambda_i + \lambda}{E\left[\tau\right]\lambda_i}\right)^2, \tag{26}$$

with $K' = 2K$.

PROOF.

Since all considered estimators have been shown to be consistent, the SINR loss is evaluated for large K by means of a perturbation analysis [32]. Starting from the perturbations on $\hat{\mathbf{R}}'$, $\hat{\mathbf{\Pi}}'_c$ and $\hat{\mathbf{\Pi}}_c^{\perp\prime}$, the SINR loss ρ of Eq. (25) is reduced in a compact form thanks to a second order approximation.

First, let us introduce the pseudo-inverse, $\mathbf{M}'$, of $\mathbf{S}'_\Sigma$ (see Eq. (12)):

$$\mathbf{M}' = \sum_{i=1}^{r}\frac{1}{E[\tau]\lambda_i}\mathbf{u}'_i\mathbf{u}_i'^H \tag{27}$$

Let $\Delta\mathbf{\Sigma}' = \hat{\mathbf{R}}' - \mathbf{\Sigma}'$ be the covariance estimation error on $\mathbf{\Sigma}'$. This estimation error induces an error on the estimates $\hat{\mathbf{\Pi}}'_c$ and $\hat{\mathbf{\Pi}}_c^{\perp\prime}$. It is shown in [32] that the projector estimates are given up to the second order with respect to $\Delta\mathbf{\Sigma}'$ by:

$$\begin{array}{rcl}\hat{\mathbf{\Pi}}'_c & \approx & \mathbf{\Pi}'_c + \delta\mathbf{\Pi}'_c + \delta^2\mathbf{\Pi}'_c \\ \hat{\mathbf{\Pi}}_c^{\perp\prime} & \approx & \mathbf{\Pi}_c^{\perp\prime} - \delta\mathbf{\Pi}'_c - \delta^2\mathbf{\Pi}'_c\end{array}, \tag{28}$$

where $\delta\mathbf{\Pi}'_c$ and $\delta^2\mathbf{\Pi}'_c$ are equal to:

$$\begin{array}{l}\delta\mathbf{\Pi}'_c = \mathbf{\Pi}_c'^{\perp}\Delta\mathbf{\Sigma}'\mathbf{M}' + \mathbf{M}'\Delta\mathbf{\Sigma}'\mathbf{\Pi}_c'^{\perp} \\ \delta^2\mathbf{\Pi}'_c = \mathbf{\Pi}_c'^{\perp}\mathbf{\Gamma}\mathbf{M}' + \mathbf{M}'\mathbf{\Gamma}^*\mathbf{\Pi}_c'^{\perp} + \mathbf{\Pi}'_c\mathbf{\Phi}\mathbf{\Pi}'_c + \mathbf{\Pi}_c'^{\perp}\Delta\mathbf{\Sigma}'\mathbf{M}'^2\Delta\mathbf{\Sigma}'\mathbf{\Pi}_c'^{\perp}\end{array} \tag{29}$$

and where matrices $\mathbf{\Gamma}$ and $\mathbf{\Phi}$ are second order terms with respect to $\Delta\mathbf{\Sigma}'$. In the following, all equalities are valid up to the second order with respect to $\Delta\mathbf{\Sigma}'$.

The second-order approximation of the denominator of Eq. (25) yields:

$$\begin{array}{l}\mathbf{d}'^H\hat{\mathbf{\Pi}}_c^{\perp\prime}\mathbf{\Sigma}'\hat{\mathbf{\Pi}}_c^{\perp\prime}\mathbf{d}' = \\ \mathbf{d}'^H\mathbf{\Pi}_c^{\perp\prime}\mathbf{\Sigma}'\mathbf{\Pi}_c^{\perp\prime}\mathbf{d}' - \mathbf{d}'^H\mathbf{\Pi}_c^{\perp\prime}\mathbf{\Sigma}'\delta\mathbf{\Pi}'_c\mathbf{d}' - \mathbf{d}'^H\delta\mathbf{\Pi}'_c\mathbf{\Sigma}'\mathbf{\Pi}_c^{\perp\prime}\mathbf{d}' + \\ \mathbf{d}'^H\delta\mathbf{\Pi}'_c\mathbf{\Sigma}'\delta\mathbf{\Pi}'_c\mathbf{d}' - \mathbf{d}'^H\delta^2\mathbf{\Pi}'_c\mathbf{\Sigma}'\mathbf{\Pi}_c^{\perp\prime}\mathbf{d}' - \mathbf{d}'^H\mathbf{\Pi}_c^{\perp\prime}\mathbf{\Sigma}'\delta^2\mathbf{\Pi}'_c\mathbf{d}'\end{array} \tag{30}$$

From Eq. (20), the first term is equal to λ. The second and the third terms are equal to 0 since $\mathbf{\Pi}_c^{\perp\prime}\mathbf{\Sigma}'\mathbf{M}' = \mathbf{0}$ and $\mathbf{M}'\mathbf{d} = \mathbf{0}$. Therefore:

$$\begin{aligned}\mathbf{d}'^H\hat{\mathbf{\Pi}}_c^{\perp\prime}\mathbf{\Sigma}'\hat{\mathbf{\Pi}}_c^{\perp\prime}\mathbf{d}' &= \lambda + \mathbf{d}'^H\delta\mathbf{\Pi}_c'\mathbf{\Sigma}'\delta\mathbf{\Pi}_c'\mathbf{d}' - 2\lambda\mathbf{d}'^H\delta^2\mathbf{\Pi}_c'\mathbf{d}' \\ &= \lambda + \mathbf{d}'^H\Delta\mathbf{\Sigma}'\mathbf{M}'\mathbf{\Sigma}'\mathbf{M}'\Delta\mathbf{\Sigma}'\mathbf{d}' - 2\lambda\mathbf{d}'^H\Delta\mathbf{\Sigma}'\mathbf{M}'^2\Delta\mathbf{\Sigma}'\mathbf{d}'.\end{aligned} \tag{31}$$

Then Eq. (12) and Eq. (27) lead to:

$$\mathbf{M}'\mathbf{\Sigma}'\mathbf{M}' = \mathbf{M}'(\mathbf{S}_\Sigma' + \lambda\mathbf{I}_m)\mathbf{M}' = \mathbf{M}' + \lambda\mathbf{M}'^2. \tag{32}$$

Now, using the previous equation, Eq. (31) becomes:

$$\mathbf{d}'^H\hat{\mathbf{\Pi}}_c^{\perp\prime}\mathbf{\Sigma}'\hat{\mathbf{\Pi}}_c^{\perp\prime}\mathbf{d}' = \lambda + \mathbf{d}'^H\Delta\mathbf{\Sigma}'\left(\mathbf{M}' - \lambda\mathbf{M}'^2\right)\Delta\mathbf{\Sigma}'\mathbf{d}'. \tag{33}$$

Secondly, let us compute the numerator of Eq. (25). We have:

$$\mathbf{d}'^H\hat{\mathbf{\Pi}}_c^{\perp\prime}\mathbf{d}' = \mathbf{d}'^H\mathbf{\Pi}_c^{\perp\prime}\mathbf{d}' - \mathbf{d}'^H\delta\mathbf{\Pi}_c'\mathbf{d}' - \mathbf{d}'^H\delta^2\mathbf{\Pi}_c'\mathbf{d}'. \tag{34}$$

Since $\mathbf{\Pi}_c^{\perp\prime}\mathbf{d}' = \mathbf{d}'$ and $\mathbf{M}'\mathbf{d}' = \mathbf{0}$, Eq. (34) is equivalent to:

$$\mathbf{d}'^H\hat{\mathbf{\Pi}}_c^{\perp\prime}\mathbf{d}' = 1 - \mathbf{d}'^H\Delta\mathbf{\Sigma}'\mathbf{M}'^2\Delta\mathbf{\Sigma}'\mathbf{d}'. \tag{35}$$

and thus:

$$\left(\mathbf{d}'^H\hat{\mathbf{\Pi}}_c^{\perp\prime}\mathbf{d}'\right)^2 = 1 - 2\mathbf{d}'^H\Delta\mathbf{\Sigma}'\mathbf{M}'^2\Delta\mathbf{\Sigma}'\mathbf{d}'. \tag{36}$$

Finally, the second order expression of the SINR loss of Eq. (25) is:

$$\rho = \lambda\frac{\left(\mathbf{d}'^H\hat{\mathbf{\Pi}}_c^{\perp\prime}\mathbf{d}'\right)^2}{\mathbf{d}'^H\hat{\mathbf{\Pi}}_c^{\perp\prime}\mathbf{\Sigma}'\hat{\mathbf{\Pi}}_c^{\perp\prime}\mathbf{d}'} = 1 - \mathbf{d}'^H\Delta\mathbf{\Sigma}'\left(\frac{1}{\lambda}\mathbf{M}' + \mathbf{M}'^2\right)\Delta\mathbf{\Sigma}'\mathbf{d}'. \tag{37}$$

As $\mathbf{M}'\mathbf{\Sigma}'\mathbf{d}' = \mathbf{0}$ (since $\mathbf{u}_i'^H\mathbf{d}' \approx 0$ for $i \leq r$), we can substitute $\hat{\mathbf{R}}'$ instead of $\Delta\mathbf{\Sigma}'$ in Eq. (37):

$$\begin{aligned}\rho &= 1 - \mathbf{d}'^H\hat{\mathbf{R}}'\left(\tfrac{1}{\lambda}\mathbf{M}' + \mathbf{M}'^2\right)\hat{\mathbf{R}}'\mathbf{d}' \\ &= 1 - \|\left(\tfrac{1}{\lambda}\mathbf{M}' + \mathbf{M}'^2\right)^{1/2}\hat{\mathbf{R}}'\mathbf{d}'\|^2\end{aligned} \tag{38}$$

Let us set:

$$\left(\frac{1}{\lambda}\mathbf{M}' + \mathbf{M}'^2\right)^{1/2} = \sum_{i=1}^{r} a_i\mathbf{u}_i'\mathbf{u}_i'^H \text{ with } a_i = \frac{1}{E\left[\tau\right]\lambda_i}\sqrt{\frac{E\left[\tau\right]\lambda_i + \lambda}{\lambda}} \tag{39}$$

and

$$\begin{aligned}\mathbf{z}_k &= \left(\tfrac{1}{\lambda}\mathbf{M}' + \mathbf{M}'^2\right)^{1/2}\mathbf{x}_k'\mathbf{x}_k'^H\mathbf{d}' \\ \mathbf{z} &= \left(\tfrac{1}{\lambda}\mathbf{M}' + \mathbf{M}'^2\right)^{1/2}\hat{\mathbf{R}}'\mathbf{d}' = \tfrac{1}{K'}\sum_{k=1}^{K'}\mathbf{z}_k\end{aligned}, \tag{40}$$

with $K' = 2K$. One has:

$$\rho = 1 - \|\mathbf{z}\|^2 \tag{41}$$

For large K', as assumed in this paper, the central limit theorem ensures that $\mathbf{z}$ is Gaussian distributed. Its first and second order moments follow from those of $\mathbf{z}_k$ and will be now investigated. The SINR loss distribution will be obtained from these results. The first order moment of $\mathbf{z}_k$ is:

$$\begin{aligned} E\left[\mathbf{z}_k\right] &= \mathcal{R}e\left(\left(\tfrac{1}{\lambda}\mathbf{M}' + \mathbf{M}'^2\right)^{1/2} E\left[\mathbf{x}'_k \mathbf{x}'^H_k\right] \mathbf{d}'\right) \\ &= \mathcal{R}e\left(\left(\tfrac{1}{\lambda}\mathbf{M}' + \mathbf{M}'^2\right)^{1/2} \mathbf{\Sigma}' \mathbf{d}'\right) = \mathbf{0}, \end{aligned} \tag{42}$$

since $\mathbf{u}'^H_i \mathbf{d}' = 0$ for $i \leq r$. Let us derive the second order moments of $\mathbf{z}_k$. By setting:

$$\mathbf{y}_k = \left[\mathbf{u}'_1 \ldots \mathbf{u}'_r \, \mathbf{d}'\right]^H \mathbf{x}'_k. \tag{43}$$

Conditionally to τ_k, $\mathbf{x}'_k$ is complex zero-mean Gaussian and its covariance eigensystem is $\tau_k\lambda_1 + \lambda > \tau_k\lambda_2 + \lambda > \ldots > \tau_k\lambda_r + \lambda > \lambda = \ldots = \lambda$ and $\left\{\mathbf{u}'_1, \ldots, \mathbf{u}'_r, \mathbf{u}'_{r+1}, \ldots, \mathbf{u}'_m\right\}$. Consequently, each component of $\mathbf{y}_k$, conditioned on τ_k, can be written as follows:

$$\begin{aligned} (\mathbf{y}_k)_i &= \sqrt{(\tau_k\lambda_i + \lambda)\chi^1_{k,i}} \exp\left(j\theta_{k,i}\right) \quad i = 1, \ldots, r \\ (\mathbf{y}_k)_{r+1} &= \sqrt{\lambda\chi^1_{k,r+1}} \exp\left(j\theta_{k,r+1}\right) \end{aligned}, \tag{44}$$

where $\chi^1_{k,i}$ and $\chi^1_{k,r+1}$ are respectively two independent Chi-square-distributed random variables with 1 degree of freedom and where $\theta_{k,i}$ is uniformly distributed on $[0, 2\pi]$. All random variables are mutually independent. Therefore, we obtain:

$$\begin{aligned} \mathbf{z}_k &= \mathcal{R}e\left(\sum_{i=1}^{r} a_i (\mathbf{u}'^H_i \mathbf{x}'_k)(\mathbf{x}'^H_k \mathbf{d}')\mathbf{u}'_i\right) \\ &= \mathcal{R}e\left(\sum_{i=1}^{r} a_i (\mathbf{y}_k)_i (\mathbf{y}_k)^*_{r+1} \mathbf{u}'_i\right) \end{aligned} \tag{45}$$

The second order moments of $\mathbf{z}_k$ are easily computed from Eqs. (44) and (45): $E\left(\mathbf{z}_k \mathbf{z}_k^T\right) = \mathbf{0}$ and

$$E\left[\mathbf{z}_k \mathbf{z}_k^H\right] = \sum_{i=1}^{r} a_i^2 E\left[(\tau_k\lambda_i + \lambda)\lambda\chi^1_i\chi^1_{r+1}\right] \mathbf{u}'_i \mathbf{u}'^H_i, \tag{46}$$

where χ_i^1 and χ_{r+1}^1 are respectively two independent Chi-square variables with 1 degree of freedom. The SINR loss distribution follows from Eq. (41), (46) and the central limit theorem:

$$\rho = 1 - \frac{1}{K'} \sum_{i=1}^{r} \left(\frac{E[\tau]\,\lambda_i + \lambda}{E[\tau]\,\lambda_i} \right)^2 \chi_i^1 \ , \tag{47}$$

with $K' = 2K$. Taking the expectation of Eq. (47) completes the proof for $E[\rho]$. $\square$

Remark. In STAP context, the hypothesis of a strong clutter in comparison to the white Gaussian noise is often valid. In this particular case, the SINR loss of proposition 3.1 admits the simplified expression:

$$E[\rho] \approx 1 - \frac{r}{2K} \tag{48}$$

Indeed, one has $E[\tau]\,\lambda_i \gg \lambda$ for $i = 1, \ldots, r$ in the case of a strong clutter. By comparing this result to the classical result of [10, 12], one can notice that a 3dB SINR Loss is reached for $K = r$, instead of $K = 2r$ when the persymmetric structure is not taken into account ($E[\rho] \approx 1 - \frac{r}{K}$ for a classic LR-STAP filter). Moreover, let us notice that the final result does not depend on the texture τ.

The result of proposition 3.1 has been obtained by an asymptotical analysis which means that this result is valid for high values of K. In the next section, the validity of this result is investigated for small values of K by means of two SAP simulations on synthetic and real data (containing a real clutter and synthetic targets).

4. Numerical Simulations

4.1. Validation of Theoretical SINR Loss

We consider the following STAP configuration to check the theoretical SINR Loss of Eq. (26). The number of sensors is $N = 8$ and the number of coherent pulses is also $M = 8$. The center frequency and the bandwidth are respectively equal to $f_0 = 450$ MHz and $B = 4$ MHz. The radar velocity is $100\ m/s$. The inter-element spacing is $d = \frac{c}{2f_0}$ (c is the speed of light) and the pulse repetition frequency is $f_r = 600$ Hz. The clutter rank is computed from Brennan's rule [7] and is equal to $r = 15$. Therefore, the clutter has a low-rank structure since $r = 15 < NM = 64$.

The CM of the Gaussian clutter, $\mathbf{C}$, is computed using the model presented in [1]. To simulate the SIRV clutter, we choose for the texture τ a Gamma distribution with shape parameter ν and scale parameter $1/\nu$ (which results in $E[\tau] = 1$). In most simulations, the CNR is $25\ dB$. Then, we obtain $\mathbf{\Sigma}'$ of Eq. (12) by using the transformation matrix $\mathbf{T}$. The eigendecomposition of this last matrix allows to obtain eigenvalues $\lambda_1, \ldots, \lambda_r, \lambda$ and therefore the theoretical SINR Loss of Eq. (26).

In the same STAP configuration, K secondary data have been simulated. These secondary data allow us to compute the SCM $\hat{\mathbf{R}}_{SCM}$ and its persymmetric counterpart $\hat{\mathbf{R}}'$ given Eq. (16). From its eigendecomposition, the sub-optimal STAP filter $\hat{\mathbf{w}}'$ of Eq. (18) has been computed and the SINR Loss of Eq. (25) has been evaluated using 1000 trials.

The same steps are used to evaluate the numerical and theoretical SINR Loss computed from the classical LR-STAP filter based on the SCM. Theoretical result for Gaussian clutter is well known [12] and the result for SIRV clutter can be found in [14].

Figure 1 shows the numerical and the theoretical SINR losses obtained from LR-STAP filters based on SCM and persymmetric SCM for different values of K and for a shape parameter of the K-distribution $\nu = 1$. Firstly, one can notice that the numerical SINR losses are very close to the theoretical ones which validates the theoretical formula of Eq. (25). Secondly, we conclude that the LR-STAP filter based on the persymmetric SCM yields better performance than the classical LR one: since two times less secondary data are required to achieve the same performance, the Persymmetric LR-STAP filter will perform better than the classical one for the same number of secondary data. Thirdly, the simulation shows that the theoretical SINR losses are still valid in a realistic context. On Fig. 1(a), the target is far from the clutter ridge and therefore the hypothesis $\mathbf{u}_i'^H\mathbf{d}' \approx 0$ for $i = 1, \ldots, r$ is valid ($\max_{i\in\{1,r\}}(|\mathbf{u}_i'^H\mathbf{d}'|) = 0.1$). For Fig. 1(b), the target is very close of the clutter ridge and therefore the assumption to obtain the theoretical result is not valid anymore ($\max_{i\in\{1,r\}}(|\mathbf{u}_i'^H\mathbf{d}'|) = 0.5$). This allows to conclude that theoretical results are close to the numerical ones in both cases which encourages the use of our result in realistic scenarios. Moreover, the LR-STAP filter based on the persymmetric SCM yields again better performance than the classical LR one: two times less of secondary data are needed to reach the same performance.

Now, let us study the SINR Losses as a function of the heterogeneity of the LR-SIRV clutter. This is the purpose of the simulation plotted on Fig. 2. A strong heterogeneity is reached for small values of ν. We show in both sub-figures that the results of the numerical and theoretical SINR Losses are close and almost

constant until a value of ν which corresponds to a very strong heterogeneity of the LR-SIRV clutter. This value depends of the number of secondary data used for the estimation of the projector. In this context of strong heterogeneity, the number of effective cells for the subspace estimation is smaller than for a homogeneous clutter which explains that the numerical SINR loss decreases with the heterogeneity of the clutter.

On Fig. 3, the shape parameter for τ is $\nu = 1$, the number of secondary data is $K = 4r$ for LR STAP built from SCM and $K = 2r$ for LR STAP built from Persymmetric SCM. On Fig. 3(a), we study the SINR losses versus the speed of the target. We show that our theoretical result is valid until a target speed of around $2\ m/s$ ($7\ km/h$), which is a very small value for ground targets. Fig. 3(b) shows the evolution of the SINR losses as a function of the CNR. The limit of validity is around $CNR = 2\ dB$.

4.2. Real Clutter Data

The STAP data are provided by the French agency DGA/MI: the clutter is real while the targets are synthetic. The number of sensors is $N = 4$ and the number of coherent pulses is $M = 64$. The center frequency and the bandwidth are respectively equal to $f_0 = 10$ GHz and $B = 5$ MHz. The radar velocity is given by $V = 100$ m/s. The inter-element spacing is $d = 0.3$ m and the pulse repetition frequency is $f_r = 1$ kHz. For this particular STAP datacube, the clutter is fitted by our clutter data model of Eq. (3) since its statistic is shown slightly non-homogeneous [33]. The CNR is equal to 20 dB. The total number of secondary data available is $K = 408$. The clutter rank obtained from the Brennan's rule [7] is equal to $r = 45$. This value is small in comparison to the full size of clutter CM, $MN = 256$. The outputs of adaptive LR-STAP filters, $\hat{\Lambda}_{LR-SCM} = |\mathbf{d}^H \hat{\mathbf{\Pi}}_c^{\perp} \mathbf{x}|^2$ and $\hat{\Lambda}'_{LR-SCM} = |\mathbf{d}'^H \hat{\mathbf{\Pi}}_c'^{\perp} \mathbf{x}'|^2$ (new LR-STAP filter proposed in this paper), are used.

In a first scenario, a target with a signal to clutter ratio of -5 dB is present at (4 m/s, $0\,\mathrm{deg}$, cell 256). Figures 4 and 5 show results of $\hat{\Lambda}_{LR-SCM}$ and $\hat{\Lambda}'_{LR-SCM}$ for respectively 100 (almost $2r$) and 50 (almost r) secondary data. As expected in the theoretical section, we notice that the persymmetry property allows to reduce the number of secondary data. On Fig. 5-(a), the target is embedded in a noise for which the level is around -130 dB while on Fig. 5-(b), the target is easily detected because the noise level has been strongly reduced, around-136 dB.

In a second scenario, 10 targets with a signal to clutter ratio of -5 dB are present at ($0\,\mathrm{deg}$, cell 252) for different speeds before and after the clutter ridge. Figures 6 and 7 show results of $\hat{\Lambda}_{LR-SCM}$ and $\hat{\Lambda}'_{LR-SCM}$ for respectively 100

(almost $2r$) and 50 (almost r) secondary data. As previously, the persymmetry property strongly enhances the performance of the LR-STAP filters. As shown the noise (clutter plus white Gaussian noise) is strongly reduced by using the persymmetry property in the derivations. There is a reduction of the level noise of almost 6 dB for some parts of the ridge clutter. Moreover, one can notice that it is more difficult to distinguish the ten targets on Fig. 7-(a) than on Fig. 7-(b).

5. Conclusion

In this paper, a new LR-STAP filter has been proposed by taking into account the persymmetry property of the CM. This filter has been derived by using both data transformed by a unitary matrix $\mathbf{T}$ and the persymmetric MLE of the CM derived in [28, 29]. Then, this filter has been theoretically analyzed through the derivation of its SINR loss. Finally, in a context of a LR-SIRV clutter, the resulting STAP filter is shown, both theoretically and experimentally, to exhibit good performance with fewer secondary data: 3dB SINR loss is achieved with only r secondary data.

Acknowledgment

We thank the French DGA/MI Agency for providing us the STAP Data set.

References

[1] J. Ward, Space-Time Adaptive Processing for airborne radar, Tech. rep., Lincoln Lab., MIT, Lexington, Mass., USA (December 1994).

[2] E. Conte, M. Bisceglie, C. Galdi, G. Ricci, A procedure for measuring the coherence length of the sea texture, IEEE Trans. on Instrumentation and Measurement 46 (4) (1997) 836–841.

[3] J. Billingsley, A. Farina, F. Gini, M. Greco, L. Verrazzani, Statistical analyses of measured radar ground clutter data, IEEE Trans. on Aero. and Elec. Syst. 35 (2) (1999) 579 – 593.

[4] K. Yao, A representation theorem and its applications to spherically invariant random processes, IEE Trans. on Inf. Th. 19 (5) (1973) 600 – 608.

[5] J. Billingsley, Ground clutter measurements for surface-sited radar, Tech. Rep. 780, MIT (February 1993).

[6] E. Conte, A. D. Maio, C. Galdi, Statistical analysis of real clutter at different range resolutions, IEEE Trans. on Aero. and Elec. Syst. 40 (3) (2004) 903 – 918.

[7] L. E. Brennan, F. Staudaher, Subclutter visibility demonstration, Tech. rep., RL-TR-92-21, Adaptive Sensors Incorporated (March 1992).

[8] M. Rangaswamy, F. Lin, K. Gerlach, Robust adaptive signal processing methods for heterogeneous radar clutter scenarios, Signal Processing 84 (2004) 1653 – 1665.

[9] I. Reed, J. Mallett, L. Brennan, Rapid convergence rate in adaptive arrays, IEEE Trans. on Aero. and Elec. Syst. AES-10 (6) (1974) 853 – 863.

[10] I. Kirsteins, D. Tufts, Adaptive detection using a low rank approximation to a data matrix, IEEE Trans. on Aero. and Elec. Syst. 30 (1994) 55 – 67.

[11] A. Haimovich, The eigencanceler: Adaptive radar by eigenanalysis methods, IEEE Trans. on Aero. and Elec. Syst. 32 (2) (1996) 532 – 542.

[12] A. Haimovich, Asymptotic distribution of the conditional signal-to-noise ratio in an eigenanalysis-based adaptive array, IEEE Trans. on Aero. and Elec. Syst. 33 (1997) 988 – 997.

[13] C. Peckham, A. Haimovich, T.F.Ãyoub, J. Goldstein, I. Reed, Reduced-rank STAP performance analysis, IEEE Trans. on Aero. and Elec. Syst. 36 (2) (2000) 664 – 676.

[14] G. Ginolhac, P. Forster, F. Pascal, J. Ovarlez, Performance of two low-rank STAP filters in a heterogeneous noise, IEEE Trans. on Sig. Proc. 61 (1) (2013) 57 – 61.

[15] H. Belkacemi, S. Marcos, Fast iterative subspace algorithms for airborne stap radar, EURASIP Journal on Applied Signal Processing ID 37296 (2006) 1–8.

[16] M. Shen, D. Zhu, Z. Zhu, Reduced-rank space-time adaptive processing using a modified projection approximation subspace tracking deflation approach, IET Radar, Sonar and Navig. 3 (1) (2009) 93 – 100.

[17] J. Goldstein, I. Reed, L. Scharf, A multistage representation of the wiener filter based on orthogonal projections, IEEE Trans. on Inf. Th. 44 (7) (1998) 2943 – 2959.

[18] M. Honig, J. Goldstein, Adaptive reduced-rank interference suppression based on the multistage wiener filter., IEEE Trans. on Comm. 50 (6) (2002) 986 – 994.

[19] D. Pados, G. Karystinos, S. Batalama, J. Matyjas, Short-data-record adaptive detection, in: Proceedings of 2007 IEEE Radar Conf., USA, 2007.

[20] L. Scharf, E. Chong, M. Zoltowski, J. Goldstein, I. Reed, Subspace expansion and the equivalence of conjugate direction and multistage wiener filters, IEEE Trans. on Sig. Proc. 56 (10) (2008) 5013–5019.

[21] F. Rui, R. de Lamare, Reduced-rank stap algorithms using joint iterative optimization of filters, IEEE Trans. on Aero.and Elect. Syst. 47 (3) (2011) 1668 – 1684.

[22] F. Rui, R. de Lamare, L. Wang, Reduced-rank stap schemes for airborne radar based on switched joint interpolation, decimation and filtering algorithm, IEEE Trans. on Sig. Proc. 58 (8) (2011) 4182 – 4194.

[23] G. Ginolhac, P. Forster, J. Ovarlez, F. Pascal, Spatio-temporal adaptive detector in non-homogeneous and low-rank clutter, in: Proceedings of ICASSP, Taipei, Taïwan, 2009.

[24] K. Gerlach, M. Picciolo, Robust, reduced rank, loaded reiterative median cascaded canceller, IEEE Trans. on Aero.and Elect. Syst. 47 (1) (2011) 15 – 25.

[25] L. Cai, H. Wang, A persymmetric multiband GLR algorithm, IEEE Trans. on Aero. and Elec. Syst. 30 (3) (1992) 806–816.

[26] E. Conte, A. D. Maio, Exploiting persymmetry for CFAR detection in compound-Gaussian clutter, IEEE Trans. on Aero. and Elec. Syst. 39 (2) (2003) 719 – 724.

[27] E. Conte, A. D. Maio, Mitigation techniques for non-Gaussian sea clutter, IEEE Journal of Oceanic Engineering 29 (2) (2004) 284 – 302.

[28] G. Pailloux, P. Forster, J. Ovarlez, F. Pascal, On persymmetric covariance matrices in adaptive detection, in: Proceedings of ICASSP, Las Vegas, Nevada, USA, 2008.

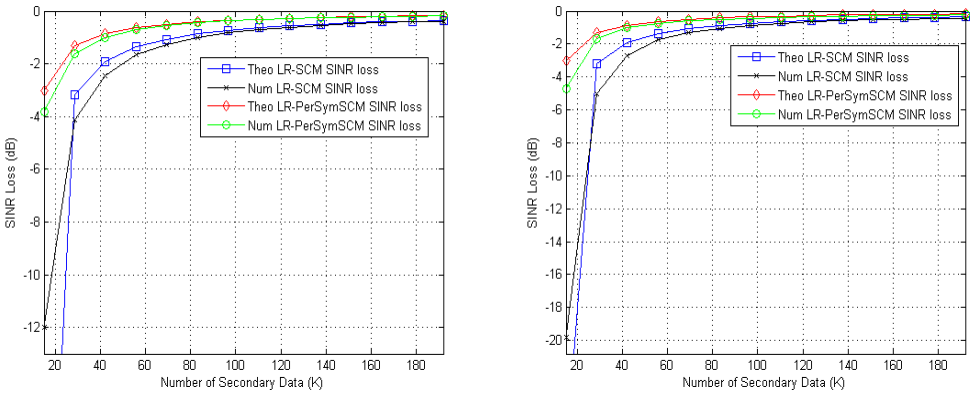
[29] G. Pailloux, P. Forster, J. Ovarlez, F. Pascal, Persymmetric adaptive radar detectors, IEEE Trans. on Aero. and Elec. Syst. 47 (4) (2011) 2376–2390.

[30] G. Ginolhac, P. Forster, F. Pascal, J. Ovarlez, Exploiting persymmetry for low-rank Space Time Adaptive Processing, in: Proceedings of EUSIPCO, Bucarest, Roumanie, 2012, pp. 81 – 85.

[31] M. Rangaswamy, D. Weiner, A. Ozturk, Non-gaussian vector identification using spherically invariant random processes, IEEE Trans.-AES 29 (1) (1993) 111–124.

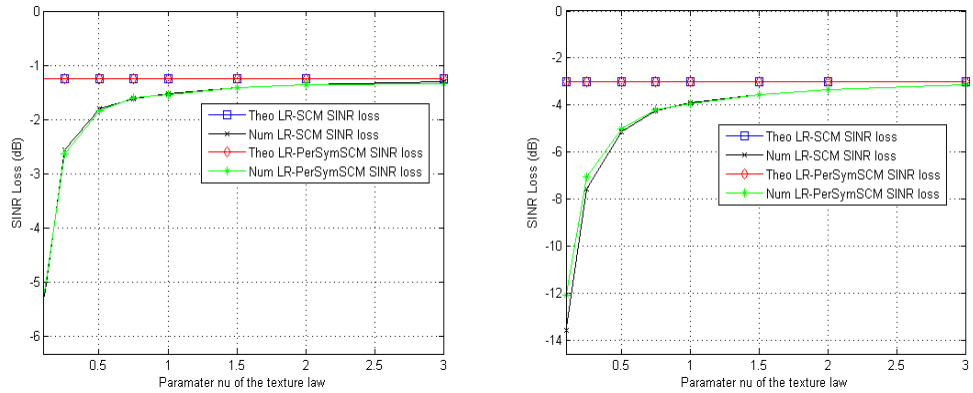
[32] H. Krim, P. Forster, J. Proakis, Operator approach to performance analysis of root-MUSIC and root-min-norm, IEEE Trans. on Sig. Proc. 40 (7) (1992) 1687 – 1696.

[33] S. Marcos, S. Beau, STAP à rang réduit, récursif en distance et utilisant un développement de taylor, Traitement du Signal 28 (1-2) (2011) 171–201.



(a) SINR Loss for a target at (40 m/s, -20 deg) (b) SINR Loss for a target at (5 m/s, 0 deg)

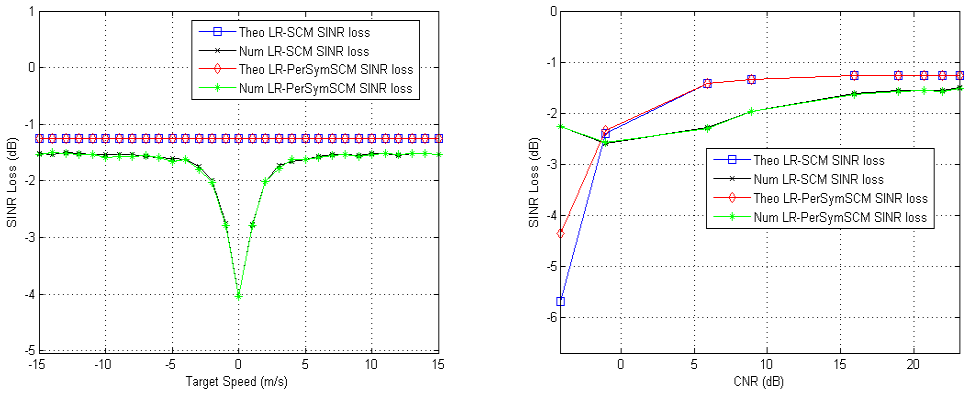
Figure 1: Theoretical SINR Loss of LR STAP built from SCM (solid line black), Numerical SINR Loss of LR STAP built from SCM (dashed line * black), Theoretical SINR Loss of LR STAP built from Persymmetric SCM (solid line red), Numerical SINR Loss of LR STAP built from Persymmetric SCM (dashed line * red) as a function of K. The shape parameter for τ is $\nu = 1$.



(a) SINR Losses of LR STAP built from SCM for $K = 4r$ and LR STAP built from Persymmetric SCM for $K = 2r$

(b) SINR Losses of LR STAP built from SCM for $K = 2r$ and LR STAP built from Persymmetric SCM for $K = r$

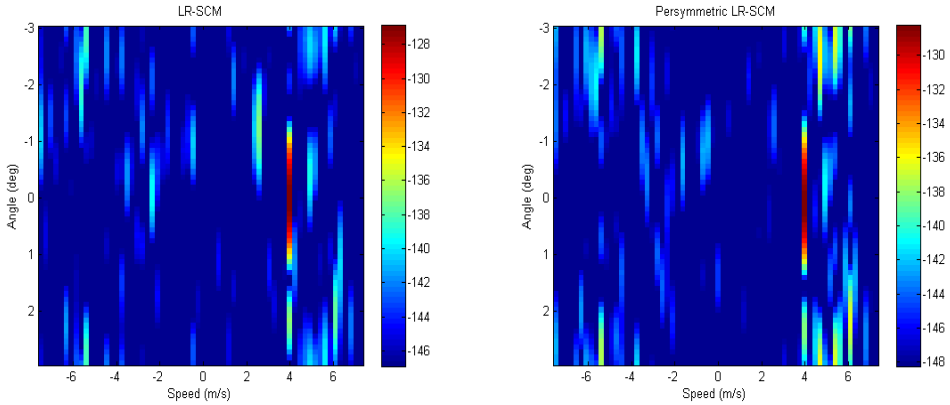
Figure 2: Theoretical SINR Loss of LR STAP built from SCM (solid line black), Numerical SINR Loss of LR STAP built from SCM (dashed line * black), Theoretical SINR Loss of LR STAP built from Persymmetric SCM (solid line red), Numerical SINR Loss of LR STAP built from Persymmetric SCM (dashed line * red) as a function of the shape parameter for τ, ν. The target is at (40 m/s, -20 deg).



(a) SINR Loss as a function of Vt. The CNR is $25\ dB$.

(b) SINR Loss as a function of CNR. The target is at $(40$ m/s, $-20\,\mathrm{deg})$.

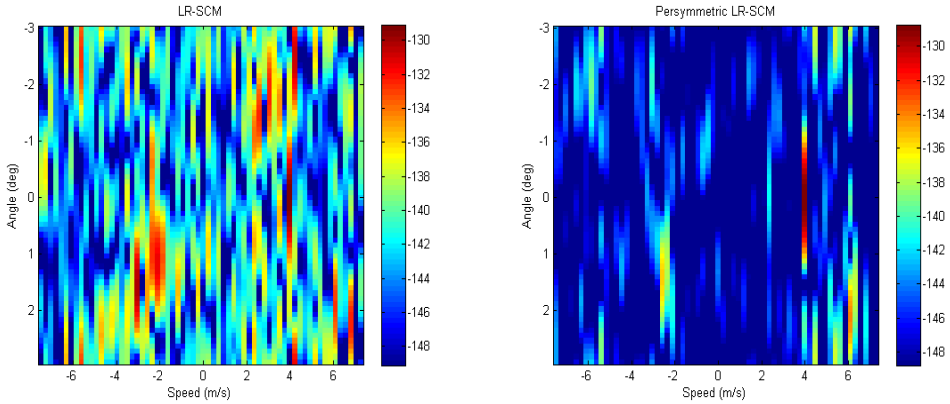
Figure 3: Theoretical SINR Loss of LR STAP built from SCM (solid line black), Numerical SINR Loss of LR STAP built from SCM (dashed line * black), Theoretical SINR Loss of LR STAP built from Persymmetric SCM (solid line red), Numerical SINR Loss of LR STAP built from Persymmetric SCM (dashed line * red). The shape parameter for τ is $\nu = 1$. $K = 4r$ for LR STAP built from SCM. $K = 2r$ for LR STAP built from Persymmetric SCM.



(a) $\hat{\Lambda}_{LR-SCM}$

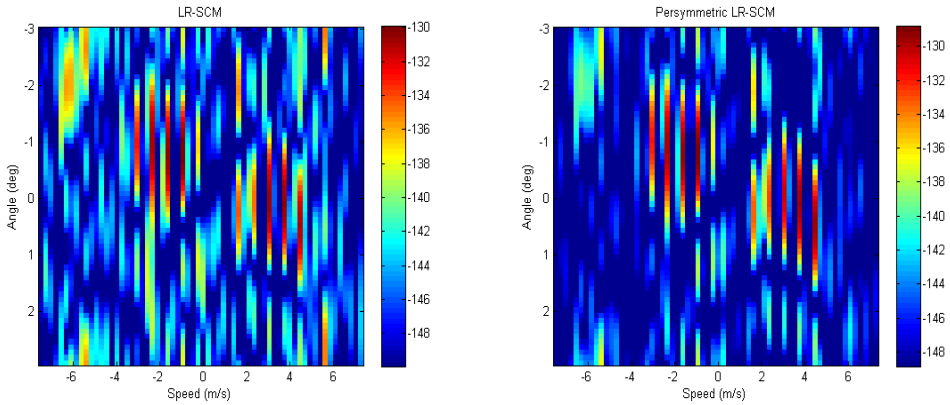
(b) $\hat{\Lambda}'_{LR-SCM}$

Figure 4: LR-STAP outputs with 100 cells to estimate the CM. Cell under test contains a target at $(4$ m/s, $0\,\mathrm{deg})$



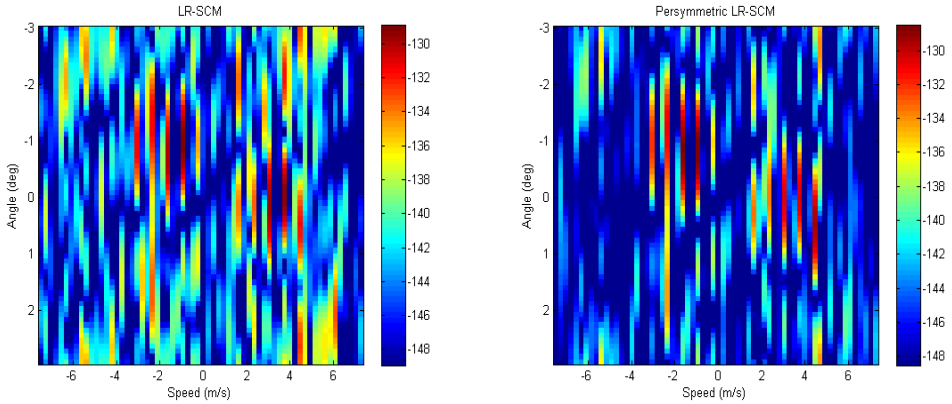
(a) $\hat{\Lambda}_{LR-SCM}$ (b) $\hat{\Lambda}'_{LR-SCM}$

Figure 5: LR-STAP outputs with 50 cells to estimate the CM. Cell under test contains a target at (4 m/s, 0 deg)



(a) $\hat{\Lambda}_{LR-SCM}$ (b) $\hat{\Lambda}'_{LR-SCM}$

Figure 6: LR-STAP outputs with 100 cells to estimate the CM. Cell under test contains ten targets at (0 deg)



(a) $\hat{\Lambda}_{LR-SCM}$ (b) $\hat{\Lambda}'_{LR-SCM}$

Figure 7: LR-STAP outputs with 50 cells to estimate the CM. Cell under test contains 10 targets at $(0\,\mathrm{deg})$